International Scholarly Research Network
ISRN Spectroscopy
Volume 2012, Article ID 634571, 7 pages
doi:10.5402/2012/634571

Research Article

Spectroscopic and Physical Properties of Bi_2O_3-B_2O_3-ZnO-Li_2O Glasses

Shashidhar Bale and Syed Rahman

Department of Physics, Osmania University, Hyderabad, 500007, India

Correspondence should be addressed to Shashidhar Bale, sss_bale@yahoo.co.in

Received 7 December 2011; Accepted 18 January 2012

Academic Editor: M. Ivanda

Bismuth glasses containing ZnO and Li_2O were prepared by conventional melt-quench technique. ZnO is gradually substituted by Li_2O, and its effect on various physical, thermal, and electrical conduction properties was studied and analyzed. Raman studies revealed that these glasses are mainly made up of $[BiO_3]$ and $[BiO_6]$ units. The density decreases and molar volume increases with the incorporation of Li_2O into these glasses. MDSC studies have been performed on these glasses to determine the glass transition temperature and other related thermal parameters such as change in the glass transition temperature (ΔT_g) and specific heat capacity difference (ΔC_p). These studies revealed that the glasses possess high T_g values, and T_g decreases with Li_2O content. The trend of these properties is attributed to the changes in the glass network structure. Dc electrical conductivity revealed that the conductivity increases and activation energy decreases with Li_2O content.

1. Introduction

The glassy materials have become increasingly important in the field of solid state ionics. They are of technological interest because of their various applications in solid state batteries, cathode ray tube, flat panel display, thick-film hybrid integrated circuits, magnetic heads, and so forth. In recent years, bismuth borate glasses [1–6] attracted the attention of researchers due to their useful physical properties, their important applications in the field of glass ceramics, thermal and mechanical sensors, reflecting windows, and so forth. A survey of the literature shows that there are many reports available on ternary bismuth borate glasses [7–11]. Recently, attention has been given to the investigation of glasses containing transition metal cations. The structural investigation of such glasses is essential to obtain a better insight into their structure-property relations. Especially, zinc-oxide-based glasses/ceramics have special applications in the areas of varistors, dielectric layers, and transparent dielectric and barrier ribs in plasma display panels [12, 13]. Furthermore, ZnO can be made versatile material with broad applications through a proper doping process such as transparent-conducting electrodes (doped with group IIIB, fluorine, and aluminum) and piezoelectric as well as ferroelectric layers [14]. Very recently structural [15], thermal, and electronic polarizability [16] studies on Bi_2O_3-ZnO-based glasses were reported.

In the present paper, we report the spectral and physical properties of Bi_2O_3-B_2O_3-ZnO-Li_2O glasses. The presence of Bi_2O_3, a conventional glass former, and B_2O_3, a classical glass former, increases the interest in the present study. The influence of ZnO and Li_2O on various properties is discussed.

2. Experimental Details

2.1. Glass Preparation. Glass samples of composition $50Bi_2O_3$-$15B_2O_3$-$(35\text{-}x)$ZnO-xLi_2O ($0 \leq x \leq 20$) were prepared by conventional melt-quench technique using reagent grade chemicals Bi_2O_3, B_2O_3, ZnO, and Li_2O (with purity more than 99%). The mixture of powders taken in a porcelain crucible was heated at 450°C for one hour to evaporate the moisture if any. The mixture was melted at a temperature of 1100–1200°C depending on the composition. The melt was then rapidly quenched in air between two highly polished steel blocks maintained at 200°C. This

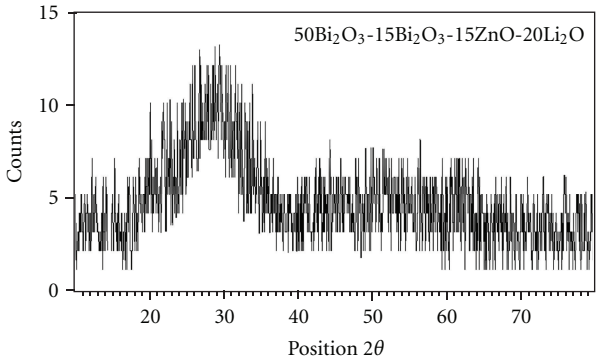

Figure 1: X-ray diffractograms of the present glasses.

gave the transparent glasses with shining surfaces. The glass samples were annealed at 200°C to remove thermal stress and strain (if any) during formation. The glass composition mentioned is the nominal composition (the starting mixture).

2.2. Glass Characterization. A small amount of the glass was powdered for the X-ray diffraction studies, and a PANalytical X-pert PRO model with Cu-K Alpha radiation (λ = 1.54048 Å) was used. The glassy phase of the samples was confirmed from XRD pattern (Figure 1) as it showed a broad hump at $2\theta \sim 30°$.

The room temperature Raman measurements were performed in the range of 100–1700 cm^{-1} on a micro-Raman system from Jobin-Yvon Horiba (LABRAM HR-800) spectrometer. The system is equipped with high-stability confocal Microscope for Micro-Raman 10x, 50x, 100x objective lens to focus the laser beam. Ar^+ laser beam of 488 nm (E = 2.53 eV) was used for excitation. The incident laser power is focused in a diameter of ~1-2 μm, and a notch filter is used to suppress Rayleigh light. In the present system, Raman shifts are measured with a precision of ~0.3 cm^{-1}.

The density (ρ) of the glass samples was determined using Archimedes principle, by using xylene (ρ = 0.86 g/cc) as the working fluid. The molar volume (V_m) has been determined as M/ρ, where M is the molar weight of the glass calculated by multiplying $\times$ times the molecular weights of the various constituents. Also, the values of the packing density $D_o = (\rho/M)\times$ number of oxygen atoms per formula unit were calculated. Li^+ concentration (N) and interionic distance (R) were also evaluated.

The glass transition temperature, T_g, was measured in all samples using a temperature-modulated differential scanning calorimeter (TA Instruments, DSC 2910). All samples were heated at the standard rate of 10°C min^{-1} in aluminum pans.

The electrical measurements were made on pure samples by the usual technique of two electrodes method. Silver paste was painted on the polished circular disc surface of the samples with thickness of ~1 mm and ~10 mm diameter. With painted silver paste, good ohmic contacts were found. The electrical conductivity was measured as a function of temperature from 200°C up to below glass transition temperature of the respective glass sample. The sample was loaded in a cylindrical furnace using a spring. The dc electrical conductivity measurements were made using a Keithley electrometer model 614. The temperature of the specimen was recorded with a chromel-alumel thermocouple kept in close thermal contact with the specimen surface.

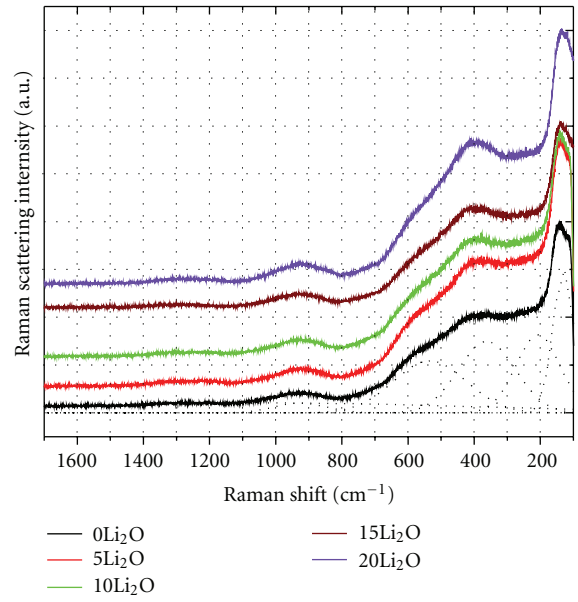

Figure 2: Effect of composition on Raman spectra.

3. Results and Discussion

3.1. Raman Spectra. Figure 2 shows the effect of composition on the Raman spectra of the studied glasses consisting of broad peaks in the range of 100–1700 cm^{-1}. The broadening of peaks is due to the disorderness in the glass matrix. To find out the exact mode of vibrations and also the Raman shifts, the spectrum with superimposed broad peaks was deconvoluted into six peaks using a Gaussian distribution (dotted curves). The peak position and the peak width of the Raman spectra thus determined for all the glasses are presented in Table 1. Vibrational spectra of Bi_2O_3 and derivatives studied by Raman spectroscopy [17] indicated that bismuth does not form a simple structure. However, it is well known that bismuth ions can form [BiO_3] pyramidal or [BiO_6] octahedral units [18–20]. Pyramidal units have four fundamental vibrations, which are all Raman active, while octahedral units have six modes of vibrations, three of which are Raman active [21]. In the present investigation, the Raman spectra are dominated by the bands associated to the structural vibrations of the heaviest cation, Bi^{3+}. The dominating peak around 130 cm^{-1} in all the spectra is an evidence for the presence of [BiO_6] octahedral and [BiO_3] pyramidal units. The bands in the range of 300–600 cm^{-1} can be assigned to symmetric stretching anion motion (~i.e., vibration of bridging oxygen) in an angularly constrained Bi–O–Bi configuration [22].

Table 1: Peak position (cm^{-1}), width (cm^{-1}), and height of the Raman spectra of the $50Bi_2O_3$-$15B_2O_3$-(35-x)ZnO-xLi_2O glass system (P: peak position, W: peak width).

$x = 0$						
P	130	220	390	555	927	1234
W	62	132	174	220	156	233
$x = 5$						
P	129	224	395	539	920	1213
W	61	140	170	186	187	198
$x = 10$						
P	130	26	387	535	925	1229
W	58	135	174	214	183	201
$x = 15$						
P	129	230	380	529	929	1220
W	83	100	171	216	160	195
$x = 20$						
P	130	234	374	524	920	1272
W	183	112	158	205	175	168

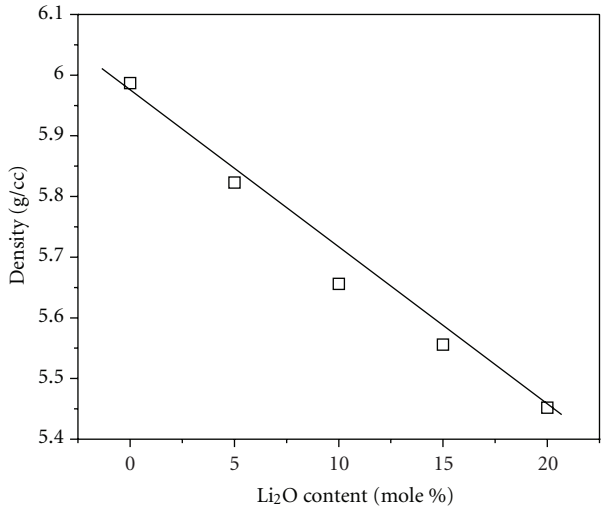

Figure 3: Variation of density with Li_2O content.

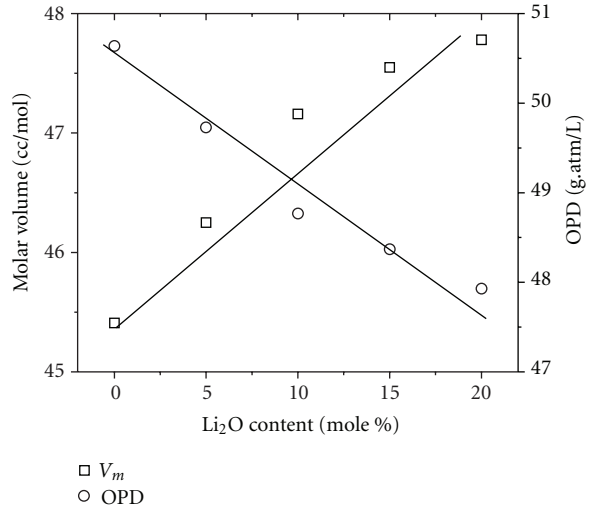

Figure 4: Variation of molar volume and oxygen packing density with composition (the solid lines are guide to eye).

The broad but strong band occurring in the present Raman spectra around 390 cm^{-1} can be attributed to the Bi–O–Bi vibrations of [BiO_6] octahedral units. It can be observed that the peak position shifts towards lower wave number with Li_2O content. This can be assumed due to the presence of lithium ions near the [BiO_6] octahedra which in turn shortens the Bi–O bonds and hence increases the energy for vibration [23]. The shoulder at 555 cm^{-1} can be attributed to $Bi–O^-$/Bi–O–Zn stretching vibrations [22]. The band at 555 cm^{-1} increases in intensity with the increase in the ZnO content. In the present glass system, B_2O_3 is constant at 15 mol%. Only orthoborate and pyroborate units may exist [24]. Therefore, in the present glass system, the Raman band around 927 cm^{-1} is due to orthoborate groups, and a very weak broad band around 1234 cm^{-1} is due to pyroborate groups. The presence of Raman peak at 220 cm^{-1} indicates the presence of Zn–O tetrahedral bending vibrations of ZnO_4 units in the present glass system [20, 25]. The Raman band assignments are presented in Table 2.

3.2. Density and Related Parameters. The density is perhaps the most important measure of a glass. Its value is needed in manifold techniques such as neutron, electron, and X-ray scattering. Density also stands on its own as an intrinsic property capable of casting light on short-range structure. The density is generally affected by the structural softening/compactness, change in geometrical configuration, coordination number, crosslink density, and dimension of interstitial spaces of the glass [26]. Figure 3 shows the variation of density with Li_2O content. It is observed that the density decreases linearly from 5.98 g/cc to 5.45 g/cc with the increase in Li_2O content. Figure 4 shows the variation of V_m as well as OPD with Li_2O content. It is noted that the V_m

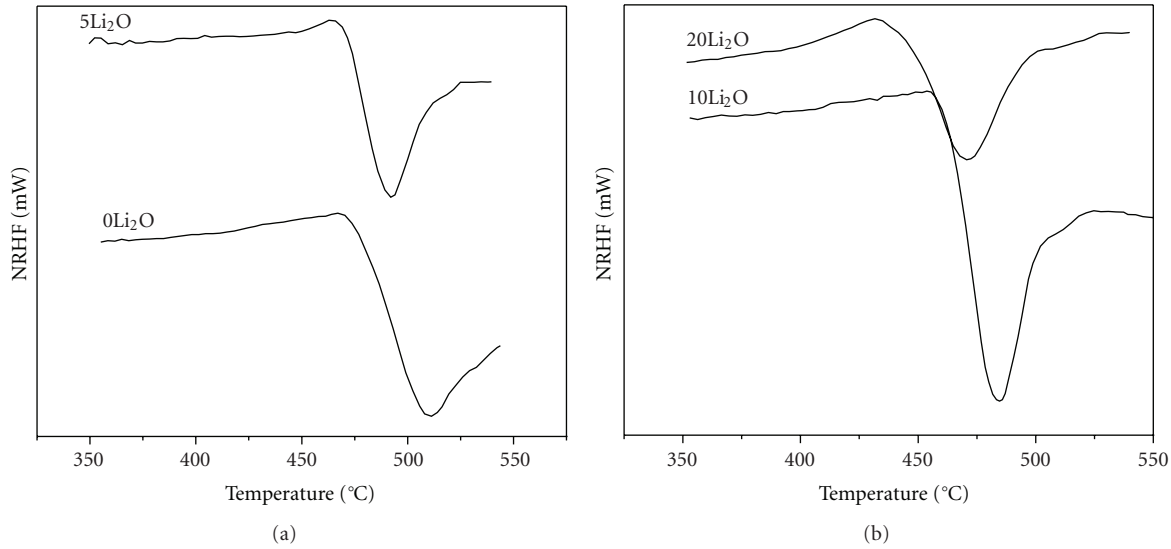

Figure 5: MDSC thermograms of the present glasses.

Table 2: Raman band assignments of the present glasses.

Peak position (cm^{-1})	Raman assignments
~130	$[BiO_3]$ and $[BiO_6]$ groups
~254	ZnO_4 groups
~390	Bi–O–Bi vibrations of $[BiO_6]$ octahedral units
~555	$Bi–O^-$ of $[BiO_6]$ groups
~927	Isolated orthoborate group
~1234	Stretching of the terminal $B–O^-$ bonds of pyroborate units

increases and OPD decreases with Li_2O content. The decease in density with Li_2O is obvious since it is being replaced by heavier ZnO.

3.3. MDSC. It is a known fact that the glass transition temperature (T_g) is a measure of structural relaxation. If a material shows the phenomenon of structural relaxation, we speak of a glass. Structural relaxation is defined by the existence of a well-defined temperature interval, the "glass-transition region," where, due to the onset of long-range atomic and molecular motion, mechanical and thermodynamic properties become time dependent. The onset of molecular motion manifests itself in a dramatic increase of the heat capacity, which is easily detected by differential scanning calorimetry.

The MDSC thermograms of the present glasses are shown in Figures 5(a) and 5(b). Figure 6 shows the heat capacity signals of the present glass samples. In DSC experiments, glass transition process shows up as an upward jump in heat capacity (C_p) baseline, and the enthalpic relaxation process accompanying it exhibits an endothermic peak in the heat flow. Since in MDSC these two signals are independently

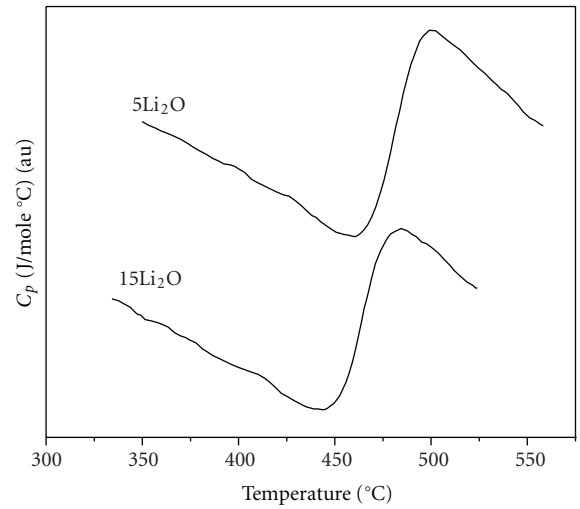

Figure 6: Heat capacity signals of the present glasses.

obtained, heat capacity and nonreversible heat flow (NRHF) are the two raw signals of interest. Therefore, it enables the accurate determination of the point of inflexion, the point where dC_p/dT attains a maximum value (Figure 7). We have used this definition to determine the value of T_g. The errors in T_g measurements in determination from the point of inflexion are found to be ± 1 K. The method of evaluation of various thermodynamical parameters such as glass transition temperature T_g, specific heat capacity C_p, change in the transition temperature ΔT_g, and specific heat capacity difference ΔC_p is reported earlier [6].

Figure 8 shows the variation of T_g with glass composition. As can be seen from the figure, the range in T_g in this study is from 454 to 491°C. That means that these glasses are stable at high temperatures up to 450°C and

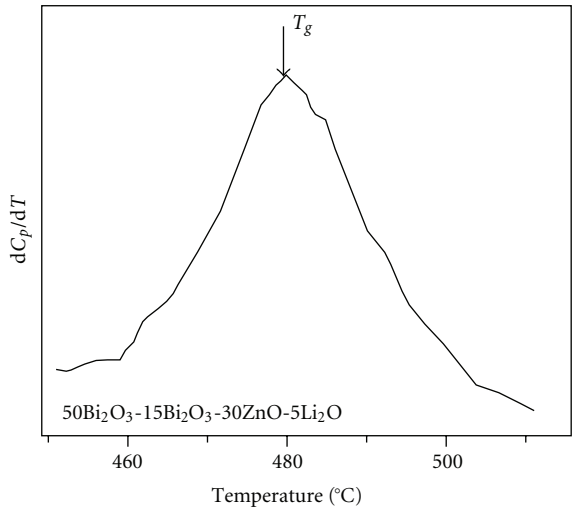

Figure 7: Derivative of heat capacity signal (dC_p/dT) versus temperature to determine glass transition temperature.

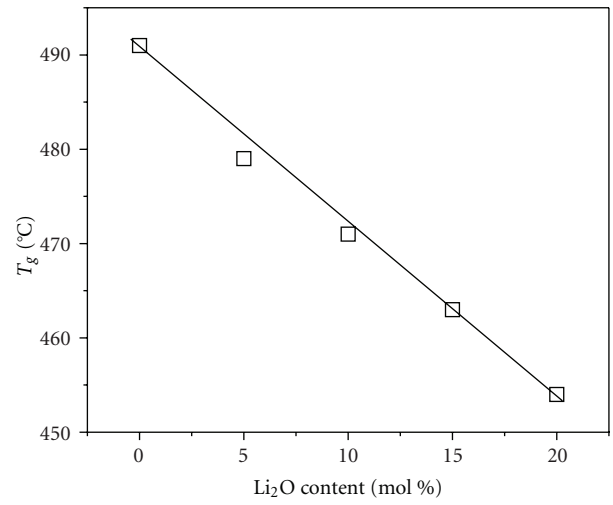

Figure 8: Variation of (T_g) with composition (the solid line is guide to eye).

can be used for various high-temperature applications. Glass transition temperatures of bismuth-based glasses have been reported previously [27, 28] in which the T_g values are much lower than the present glasses. The high glass transition temperature of the present glasses can be attributed due to the presence of ZnO. From the figure, it is also evident that the glass transition temperature decreases and shows a tendency of linear relationship with Li_2O content. It is considered that T_g depends on the strength of the chemical bond, crosslink density in the glass structure. In general, the incorporation of alkaline metals at lower concentration into a base glass network (borate, silicate, bismuthate, etc.) plays a role of network modifier due to which the number of nonbridging oxygen increases. This results in the decrease in the crosslink density, loosening the glass network. It is widely known that the bond between alkaline atom and oxygen is ionic bond which is in general weaker than the covalent bond. Hence, in the present study, T_g decreases with the increase in Li_2O content. This result is supported by the density measurements, where the molar volume increases with Li_2O content.

The values of C_p, ΔC_p, T_g, and ΔT_g for the present glasses are given in Table 3. For all samples, the smaller values of ΔC_p are an indication of strong resistance to any structural change, showing that the glass-forming liquid has a number of configurational degrees of freedom associated with it.

3.4. DC Electrical Conductivity. The reciprocal temperature dependence of the dc conductivity for different compositions is shown in Figure 9. The figure shows that the plots are straight lines indicating that the dc conductivity obeys the Arrhenius relation

$$\sigma_{\mathrm{dc}} = \sigma_o \exp\left(-\frac{E_{\mathrm{dc}}}{kT}\right), \tag{1}$$

where E_{dc} is the thermal activation energy, k is the Boltzmann constant, σ_o is the preexponential factor, and T is the absolute temperature. It can be observed from the figure that the electrical conductivity increases with lithium content and also with temperature. The activation energy E_{dc} has been calculated for different compositions from least square straight line fits of Arrhenius plots. The variation of dc conductivity at a particular temperature and the activation energy with Li_2O content are presented in Figure 10. It can be noted from the figure that the dc conductivity increases and the activation energy decreases with Li_2O content.

As Li_2O (which acts as a network modifier) is added, the base glass network is modified by the formation of more and more nonbridging oxygen ($Bi–O^-–Li^+$). These kinds of entities create a large number of charge carriers Li^+ which can easily move through the glass during heating. This fact contributes to the increase of electrical conduction. On the other hand in the other way, when ZnO replaces Li_2O, Bi–O–Zn bonds are formed along with a stronger covalent Bi–O bonds which are stronger than Li^+–O one. This is in accordance with the increase of glass transition temperature and decrease of the molar volume with ZnO. Similar results were reported previously [6, 29].

Table 3: Physical parameters of the glass system $50Bi_2O_3$-$15B_2O_3$-(35-x)ZnO-xLi_2O.

Parameter	$x = 0$	$x = 5$	$x = 10$	$x = 15$	$x = 20$
Avg·mol·wt.	271.9	269.3	266.7	264.1	261.1
N ($\times 10^{21}$)/cc	—	1.30	2.55	2.80	5.02
R (Å)	—	9.16	7.31	6.40	5.84
ΔT_g (°C)	25.8	26.5	43.8	25.5	22.8
C_p (J/mol°C)	27.2	23.6	19.5	33.2	34.2
ΔC_p (J/mol°C)	3.5	2.2	1.1	5.3	4.3

N: Li^+ ion concentration.
R: Li^+ ion interionic distance.

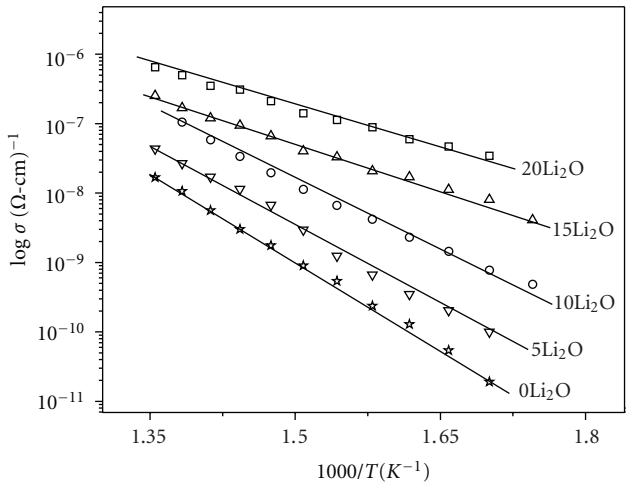

Figure 9: Plots of reciprocal dependence of conductivity of the present glasses.

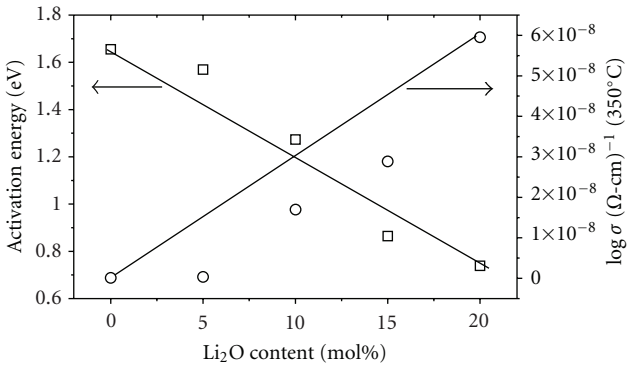

Figure 10: Variation of conductivity and activation energy with composition in the present glass system (the solid lines are guide to eye).

4. Conclusions

From the present investigation, it can be concluded that

(i) these glasses are made up of [BiO_3] and [BiO_6] units. Formation of ZnO_4 units was also observed;

(ii) the density decreased and molar volume increased with Li_2O content;

(iii) these glasses possess T_g in the range of 454–491°C. The glass transition temperature decreases with Li_2O content, which was due to the decrease of crosslink density;

(iv) the dc electrical conductivity studies revealed that the electrical conductivity increases with lithium and also with temperature and obeys Arrhenius law, whereas the activation energy decreases with Li_2O content.

References

[1] S. Rani, S. Sanghi, Anshu, A. Agarwal, N. Kishore, and V. P. Seth, "Effect of ZnO/CdO on the structure and electrical conductivity in $Li_2O{\cdot}MO{\cdot}Bi_2O_3{\cdot}B_2O_3$ glasses (M=Zn, Cd)," *Journal of Physics and Chemistry of Solids*, vol. 69, no. 7, pp. 1855–1860, 2008.

[2] A. Bajaj, A. Khanna, B. Chen et al., "Structural investigation of bismuth borate glasses and crystalline phases," *Journal of Non-Crystalline Solids*, vol. 355, no. 1, pp. 45–53, 2009.

[3] A. Dutta and A. Ghosh, "Ionic conductivity of Li_2O-BaO-Bi_2O_3 glasses," *Journal of Non-Crystalline Solids*, vol. 351, no. 3, pp. 203–208, 2005.

[4] S. Bale and S. Rahman, "Optical absorption and EPR studies on $(70 - x)Bi_2O_3$-xLi_2O_3-0(ZnO-B_2O_3) ($0 \le x \le 20$) glasses," *Journal of Non-Crystalline Solids*, vol. 355, no. 43-44, pp. 2127–2133, 2009.

[5] S. Bale, N. S. Rao, and S. Rahman, "Spectroscopic studies of Bi_2O_3-Li_2O-ZnO-B_2O_3 glasses," *Solid State Sciences*, vol. 10, no. 3, pp. 326–331, 2008.

[6] S. Bale, S. Rahman, A. M. Awasthi, and V. Sathe, "Role of Bi_2O_3 content on physical, optical and vibrational studies in Bi_2O_3-ZnO-B_2O_3 glasses," *Journal of Alloys and Compounds*, vol. 460, no. 1-2, pp. 699–703, 2008.

[7] S. Bale and S. Rahman, "Glass structure and transport properties of Li_2O containing zinc bismuthate glasses," *Optical Materials*, vol. 31, no. 2, pp. 333–337, 2008.

[8] G. Sharma, K. Singh, Manupriya, S. Mohan, H. Singh, and S. Bindra, "Effects of gamma irradiation on optical and structural properties of PbO-Bi_2O_3-B_2O_3 glasses," *Radiation Physics and Chemistry*, vol. 75, no. 9, pp. 959–966, 2006.

[9] B. Karthikeyan and S. Mohan, "Structural, optical and glass transition studies on Nd^{3+}-doped lead bismuth borate glasses," *Physica B*, vol. 334, no. 3-4, pp. 298–302, 2003.

[10] K. Singh, "Electrical conductivity of Li_2O-B_2O_3-Bi_2O_3: a mixed conductor," *Solid State Ionics*, vol. 100, no. 1-2, pp. 143–147, 1997.

[11] T. Honma, Y. Benino, T. Fujiwara, T. Komatsu, and R. Sato, "Crystalline phases and YAG laser-induced crystallization in Sm_2O_3-Bi_2O_3-B_2O_3 glasses," *Journal of the American Ceramic Society*, vol. 88, no. 4, pp. 989–992, 2005.

[12] D. R. Clarke, "Varistor ceramics," *Journal of the American Ceramic Society*, vol. 82, no. 3, pp. 485–502, 1999.

[13] M. Busio and O. Steigelmann, "New frit glasses for displays," *Glass Science and Technology*, vol. 73, no. 10, pp. 319–325, 2000.

[14] S. Fujihara, C. Sasaki, and T. Kimura, "Preparation of Al- and Li-doped ZnO thin films by sol-gel method," *Key Engineering Materials*, no. 181-182, pp. 109–112, 2000.

[15] F. He, J. Wang, and D. Deng, "Effect of Bi_2O_3 on structure and wetting studies of Bi_2O_3–ZnO–B_2O_3 glasses," *Journal of Alloys and Compounds*, vol. 509, no. 21, pp. 6332–6336, 2011.

[16] T. Inoue, T. Honma, V. Dimitrov, and T. Komatsu, "Approach to thermal properties and electronic polarizability from average single bond strength in ZnO-$Bi_2O_3B_2O_3$ glasses," *Journal of Solid State Chemistry*, vol. 183, no. 12, pp. 3078–3085, 2010.

[17] R. J. Betsch and W. B. White, "Vibrational spectra of bismuth oxide and the sillenite-structure bismuth oxide derivatives," *Spectrochimica Acta Part A*, vol. 34, no. 5, pp. 505–514, 1978.

[18] H. Zheng, R. Xu, and J. D. Mackenzie, "Glass formation and glass structure of $BiO_{1.5}$-CuO-$Ca_{0.5}Sr_{0.5}O$," *Journal of Materials Research*, vol. 4, no. 4, pp. 911–915, 1989.

[19] R. Iordanova, Y. Dimitriev, V. Dimitrov, S. Kassabov, and D. Klissurski, "Glass formation and structure in the V_2O_5-Bi_2O_3-Fe_2O_3 glasses," *Journal of Non-Crystalline Solids*, vol. 204, no. 2, pp. 141–150, 1996.

[20] S. Bale, M. Purnima, C. Srinivasu, and S. Rahman, "Vibrational spectra and structure of bismuth based quaternary

glasses," *Journal of Alloys and Compounds*, vol. 457, no. 1-2, pp. 545–548, 2008.

[21] K. Nakamoto, *Infrared and Raman Spectra of Inorganic Compounds*, John Wiley & Sons, New York, NY, USA, 1963.

[22] A. A. Kharlamov, R. M. Almeida, and J. Heo, "Vibrational spectra and structure of heavy metal oxide glasses," *Journal of Non-Crystalline Solids*, vol. 202, no. 3, pp. 233–240, 1996.

[23] M. Nocuń, W. Mozgawa, J. Jedliński, and J. Najman, "Structure and optical properties of glasses from Li_2 Bi_2O_3 PbO system," *Journal of Molecular Structure*, vol. 744, pp. 603–607, 2005.

[24] B. N. Meera and J. Ramakrishna, "Raman spectral studies of borate glasses," *Journal of Non-Crystalline Solids*, vol. 159, no. 1-2, pp. 1–21, 1993.

[25] L. Del Longo, M. Ferrari, E. Zanghellini et al., "Optical spectroscopy of zinc borate glass activated by Pr^{3+} ions," *Journal of Non-Crystalline Solids*, vol. 231, no. 1-2, pp. 178–188, 1998.

[26] H. Doweidar and Y. B. Saddeek, "FTIR and ultrasonic investigations on modified bismuth borate glasses," *Journal of Non-Crystalline Solids*, vol. 355, no. 6, pp. 348–354, 2009.

[27] J. Fu and H. Yatsuda, "New families of glasses based on Bi_2O_3," *Physics and Chemistry of Glasses*, vol. 36, no. 1-2, pp. 211–215, 1995.

[28] A. Nitta, M. Koide, and K. Matusita, "Glass formation and thermal properties of Bi_2O_3-ZnO-B_2O_3-R_2O quaternary systems," *Physics and Chemistry of Glasses*, vol. 42, no. 4-5, pp. 275–278, 2001.

[29] S. Hazra, S. Mandal, and A. Ghosh, "Properties of unconventional lithium bismuthate glasses," *Physical Review B*, vol. 56, no. 13, pp. 8021–8025, 1997.